HAZARD, LIKE NO OTHER: sensitivity, testing, validation and optimization of manifold seismic hazard models of Italy

R.W. Romeo[1], G. Sposini[2], A. Pugliese[3] and M. Caputo[4]

[1] *GISLab, University Carlo Bo, Urbino, Italy*
[2] *RIG Group SpA, Turin, Italy*
[3] *APAT, Rome, Italy*
[4] *Department of Physics, University La Sapienza, Rome, Italy*

(Received: April 15, 2008; accepted: June 11, 2008)

ABSTRACT The results of a probabilistic seismic hazard analysis of Italy, achieved according to scientifically accepted methodologies, updated information and well-documented data processing, are shown. The hazard assessment is carried out according to Cornell's method, based on an earthquake catalogue with the foreshock and aftershock events filtered out, and on three different types of seismic sources: macro-areas, seismogenic zones and single points (seismic epicentres). Peak Ground Acceleration (PGA) and Spectral Acceleration (SA) values at two fixed frequencies (1 and 5 Hz) are computed using two sets of attenuation equations: the attenuation relationships based on strong motion recordings of Italian earthquakes and the attenuation relationships based on strong motion recordings of European earthquakes. A Poisson model of earthquake occurrence is assumed as a default and three return periods are investigated, 100, 500 and 1000 years. For validation purposes, seismic hazard estimates are then compared with those obtained by using a different seismic database and procedure. They were based on the seismic intensities felt in 2,579 municipalities, giving thus the opportunity to compare, for the same sites, the hazard obtained through two alternative methods, a direct one (felt intensities) versus a derived one (strong motion estimates). Furthermore, a panel of seismic hazard experts has been solicited to provide their relative confidence in the alternative models used in this work as far as seismic source models, seismicity rate models, and attenuation models are concerned. A sensitivity analysis has been also performed, to determine those models that mostly influence the results. A hazard model, which is a synthesis of the previous ones, is finally proposed: it represents the best fit of the results of the sensitivity analyses and validation tests.

1. Introduction

Since the second half of the 1990s, seismic hazard studies increasingly influenced the policies for a seismic risk reduction. Among others, policies of fiscal deductions promoting the reduction of buildings' vulnerability in highly seismic areas (OPCM 2788, 1998), or new seismic zoning of the country (OPCM 3274, 2003) and design seismic rules (NTC, 2005) are worthy of mention. In the meantime, the research evolved from the first studies with the seismotectonic approach (Slejko *et al*., 1998) to the first sensitivity studies (Romeo and

Pugliese, 2000) and the incorporation of site effects (Romeo *et al*., 2000), until the consensus studies (Albarello *et al*., 2000) and the logic-tree analyses (MPS04, 2004). Each of these approaches explored partial aspects of hazard, starting however from the common consideration that, owing to the lack of observed data on seismic shaking, the hazard had to be assessed with an indirect approach [from sources to sites, see Reiter (1990)] depending on three fundamental matters: Where and When earthquakes happen, and How their effects propagate?

Each of these questions does not obviously have a univocal answer since they depend on a fundamental question: what is the reference seismicity?

In a seismicity model that is primarily based on seismological data rather than on geodynamic or rheological ones, the choice of an earthquake catalogue (Caputo, 2000) and a completeness model give the reference seismicity. In this sense, the catalogue represents the Universe and the completeness model the Reference System within which the laws that regulate the phenomenon, that is, the Hazard are determined:

$$\text{Hazard} = f(\text{Reference Seismicity}) = f(\text{Universe} + \text{Reference System}) \quad (1)$$

Only once the Reference Seismicity is fixed, alternative models of seismic sources, earthquake activity and attenuation relationships can be consistently established, giving, respectively, the answer to the questions Where, When and How earthquakes occur. As a matter of fact, every seismic hazard analysis that incorporates multiple models of completeness continuously changes the Reference System, thus avoiding a consistent exploration of the epistemic uncertainties.

A convenient way of exploring the epistemic uncertainties of Hazard is given by the logic-tree analysis, provided that every branch, departing from the same node, is mutually exclusive. Each of them shall be interpreted as a different, possible, state of the nature to which a degree of judgment rather than a probability level may be attributed (Krinitzsky, 1995; Abrahamson and Bommer, 2005; Albarello, 2006). In such a way, every outcome only represents one of a set of possible scenarios.

Furthermore, the influence exerted on the Hazard by each outcome can be conveniently explored by means of a sensitivity analysis, that represents also a powerful tool of choice (and decision-making) even more than the degrees of belief themselves.

As every indirect approach needs to be validated with a direct one, so the hazard, computed with Cornell's (1968) approach (from source-to-site), has to be compared with a hazard assessed by looking at the observed shakings. Of course, the validating hazard has to be: a) independent, that means assessed with completely different data and procedures, and b) comparable, that means the two outputs can be compared with each other. Seismic hazard studies, based on the observed shakings, are strongly limited due to the lack of strong motion data, for a suitable number of sites. Nevertheless, the large amount of historical data, in Italy, makes it possible to assess the hazard on the basis of the felt intensities for a number of sites which cover about one-third of the Italian municipalities (Albarello *et al*., 2002). Finally, a best Hazard estimate is formulated consistently with the validation tests and the sensitivity analyses, taking into account all possible sources of uncertainties.

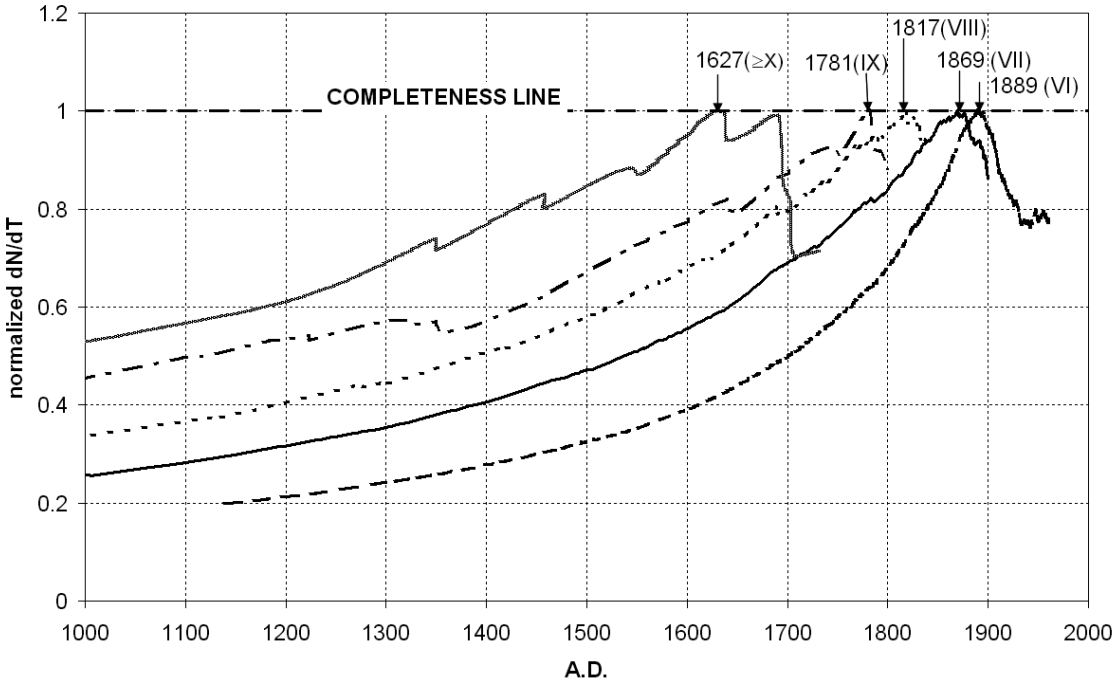

Fig. 1 - Completeness graph: the completeness interval of each intensity-magnitude class is given by the maximum derivative of the cumulative number of events.

2. Reference Seismicity

Many earthquake catalogues have been produced in Italy in the past decades. Nevertheless, if we assume that the seismicity is a stationary process, the choice strongly reduces itself to a few catalogues: among these, the most recent one is the CPTI04 (2004) catalogue, which assures a list of independent events because of the removal of foreshocks and aftershocks.

A key question in the use of historical seismicity for seismic hazard assessments is given by the completeness of the earthquake catalogue, usually based on statistical analyses or historical considerations. An engineered-seismic hazard analysis should rely on a completeness analysis that guarantees the highest activity rates. In this study, the completeness intervals have been determined by computing the derivative of the cumulative number of events versus time (Fig. 1).

For each intensity class the completeness interval begins with the highest value of the derivative (maximum); when multiple maxima are allowed, the choice reverts to the oldest one provided that no interval is longer than the interval of the successive higher intensity classes. This assures a progressive increase of the completeness intervals as the intensity increases in turn.

Table 1 shows the completeness intervals along with the intensity vs. magnitude conversion. The surface wave magnitude (M_S) has been selected since it better describes the real earthquake energy, significant for seismic hazard analyses in the magnitude range of engineering interest. A minimum magnitude M_S=4.6 has been chosen according to the threshold site intensity (*Is*=VI-

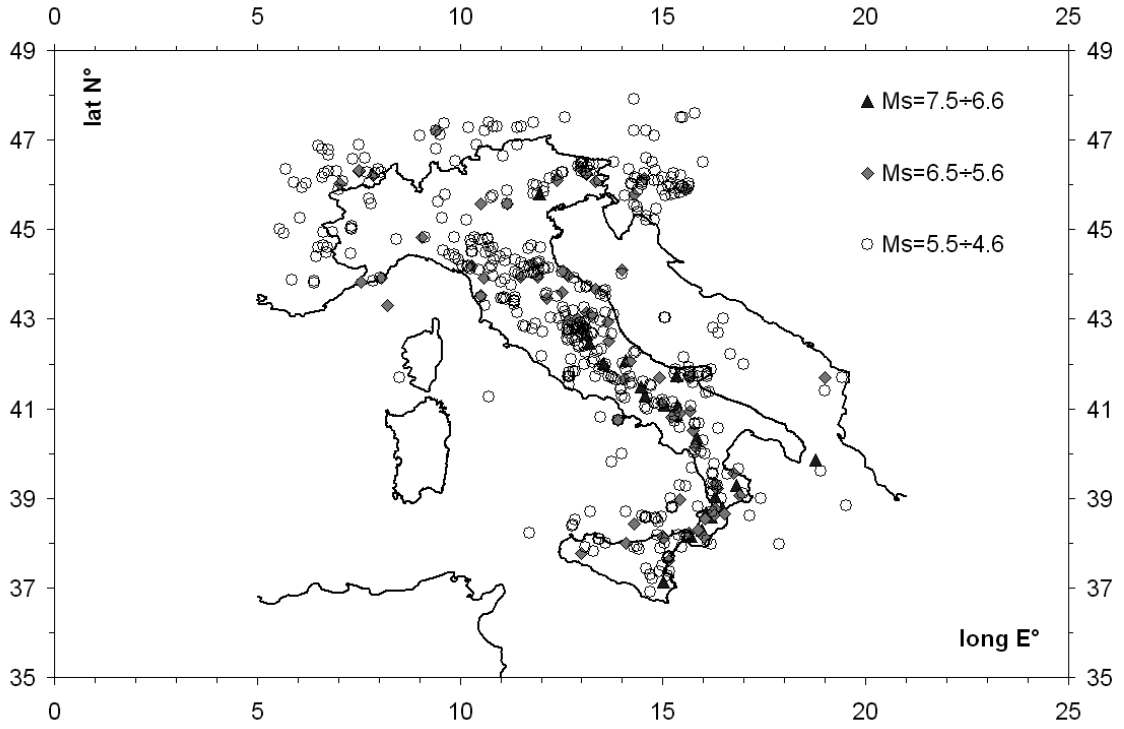

Fig. 2 - Earthquake distribution after the removal of the events falling outside the completeness intervals. These events determine the Reference Seismicity used in the hazard analyses.

VII) above which a damage level I (Orsini, 1999) may occur to type-B buildings in the MSK intensity scale.

Only 547 out of 2550 earthquakes remained after the removal of the events falling outside the completeness windows, and their spatial distribution is shown in Fig. 2.

The seismicity rate computed in this study is equal to 3.647 that means an average number of about 4 earthquakes per year above the threshold magnitude (i.e., M_S≥4.6). This is what we have called the Reference Seismicity that has been accommodated by every seismicity model described hereinafter; such a rate is preserved in each SHA carried out in this study, with an approximation of 3.647±0.001, that means, with an increase (or decrease) of only one earthquake every one thousand years at the lowest magnitude class.

Table 1 - Start-time of the completeness intervals, cumulative number of events and seismicity rate (reference seismicity) above the threshold magnitude of engineering interest (M_S=4.6).

o	VI	VI-VII	VII	VIII	IX	≥ X	N(≥VI-VII)	**N/y**
Ms	4.3	4.6	4.9	5.5	6.1	≥ 6.7	N(≥ 4.6)	
time	1889	1869	1869	1817	1781	1627	547	**3.647**

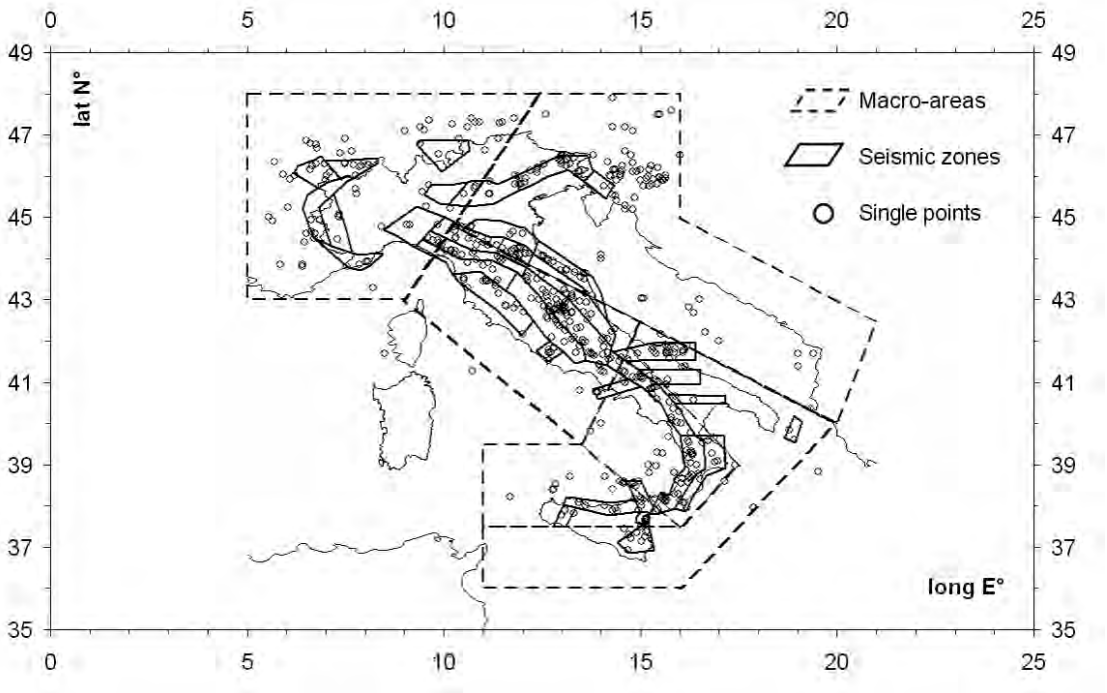

Fig. 3 - Seismic source models used in this study: dashed polygons are six macro-areas based on geodynamics; solid polygons are thirty-six seismic zones based on seismotectonics; single points are the epicentres of the complete catalogue (see figure 2).

3. Seismic sources

In the Cornell (1968) and McGuire (2004) approach, an important role is played by the geometry of the seismic sources. Thus, every seismic hazard analysis that wants to capture the epistemic uncertainty must rely on multiple seismic source models. According to the reference seismicity and the most recent studies about seismotectonics in Italy, three different models of seismic sources have been considered (Fig. 3):

a) Macro-areas (Akinci, 2004): the seismicity is included into six wide areas reflecting the different geodynamic regime of the Italian peninsula on the main basis of the different rupture mechanism (Montone *et al*., 2003), seismotectonic behaviour (Meletti *et al*., 2000), and the tectonic and geologic environment (Vai, 2001). Earthquakes are assumed to be uniformly distributed within each macro-area;

b) Seismogenic zones [ZS9: MPS04 (2004)]: the seismicity is included in 36 tectonically homogenous zones, each one reflecting the surface projection of one or more sets of faults with similar kinematical characteristics (Scandone and Stucchi, 2000; Valensise and Pantosti, 2001). Earthquakes are assumed to be uniformly distributed within every zone; a background area of diffuse seismicity is also assumed in order to include the earthquakes that a geometrically out of the source zones;

c) Single points (seismic epicentres); the epicentres of the historic earthquakes were considered as seismic sources of concentrated seismicity. In this model, ground motion

values are attenuated directly from the epicentral locations, and the seismicity rates are partitioned among the source-points according to the seismic catalogue and regional geodynamics. This model relies on the evidence that the most reliable seismic database for seismic hazard analyses in Italy is given by the earthquake catalogue itself.

The models a) and b) account for a non-stationary spatial occurrence of the seismicity, the third one implies a full stationary model of the earthquake occurrence.

4. Frequency-magnitude distributions

Two different models of magnitude distributions have been adopted in the present study: one based on magnitude distribution according to the classical Gutenberg-Richter (1944) law (GR rates); the second one, directly based on the observed magnitude distributions (AR rates). In Fig. 4, we can observe both models for the complete catalogue used for the seismic hazard. The GR fits have been computed by means of an ordinary least-squares regression analysis, because no void class is present in the investigated magnitude range.

Much information can be inferred from Fig. 4. First, frequency-magnitude relationships exhibit *b*-coefficients very close to 1, according to the theory that for large seismic regions the coefficients stand within a range of 1(±0.2). Second, the GR law tends to overestimate the largest magnitudes (above 7); indeed, this evidence which is quite common may be reduced by adopting a truncated double-exponential distribution with the same *b*-coefficient providing that the maximum magnitude be fixed to M_S=7.5 to preserve the reference seismicity (3.647 events/year). Third, in the same figure a validation test of the reference seismicity (and the completeness analysis, as well) is also shown. The seismicity rates derived from the instrumental Italian catalogue (CSI 1.1, 2006) may be considered complete in the magnitude range 4.0÷5.8. As can be seen, there is a good visual agreement between the two GR relationships; moreover, the yearly number of events in the common magnitude range 4.6÷5.8 is almost the same, being 3.72 from the CPTI04 (2004) catalogue and 3.73 from the CSI 1.1 (2006) one. For a further comparison, the MPS04 (2004) study provides a yearly number of events equal to 2.84 for the historical completeness and equal to 3.36 for the statistical completeness in the same magnitude range. Both these values are well below that pointed out by the validating instrumental catalogue, but anyway they once again confirm the superiority of the statistical methods on the historical ones to compute the completeness intervals.

5. Attenuation relationships

Two attenuation relationships are used: the set of attenuation equations proposed by Sabetta and Pugliese (1996) that are valid for the whole of Italy and the set of attenuation equations proposed by Ambraseys *et al*. (1996) that are valid for Europe. The two data sets are composed as follows:

- the Italian data set consists of 95 triaxial records generated by 17 earthquakes in Italy with a surface wave magnitude between 4.6 and 6.8 and distances up to 100 km;
- the European data set consists of 422 triaxial records generated by 157 earthquakes in Europe and adjacent regions with a surface wave magnitude between 4.0 and 7.5 and

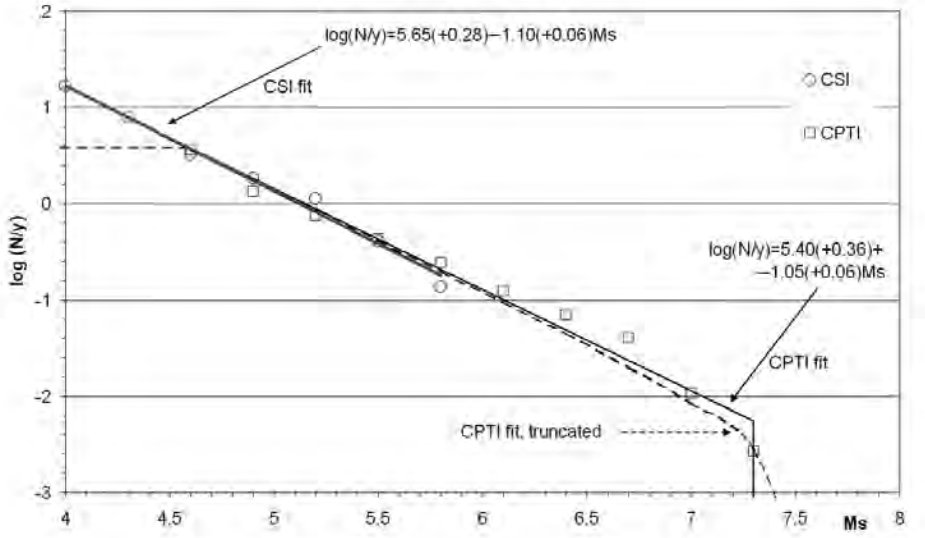

Fig. 4 - Observed rates and Gutenberg-Richter relationships for both the CPTI04 (2004) complete catalogue used in this study and the CSI 1.1 (2006) instrumental catalogue used for validation. Symbols like open squares and circles refer to observed rates (AR) for, respectively, the historical and the instrumental catalogues. Dashed line is the truncated exponential best fit of the historical data.

distances up to 200 km.

Despite the availability of a new set of attenuation equations for the European region, issued by Ambraseys *et al*. (2005), they were discarded because they make use of the moment magnitude scale. We preferred to use the previous version of the European attenuation relationships (Ambraseys *et al*., 1996) for the sake of homogeneity with the magnitude scale used by the Italian attenuation relationships, which consists of surface wave magnitude. In fact, using two different magnitude scales would have led to two different reference seismicities, thus invalidating any reliable comparison among different attenuation models. Nonetheless, the use of empirical conversions among different magnitude scales introduces a further source of uncertainty to be avoided whenever possible. The intrinsic uncertainty of the magnitude conversion between surface waves and hybrid magnitude (M_L below 5.5 and M_S above) inherent in the Italian attenuation relationships, is instead easily overcome by looking at their error bounds (Fig. 5).

Furthermore, the choice of the two attenuation relationships has been also dictated by the fact that the Italian one alone does not cover the whole magnitude-distance range over which the seismic hazard is computed. In fact, the maximum magnitude estimated by the truncated distribution is 7.5, well above the maximum magnitude used by the Italian data set (equal to 6.9). For the sake of truth, we must recognize that the two attenuations are not mutually exclusive; in fact, about 40% of the European data set includes also the strongest earthquakes contained in the Italian one. Nevertheless, in the magnitude-distance range common to both the attenuations, a different behaviour can be observed (Fig. 6).

From Fig. 6, one can infer that the role played by the Italian attenuation increases as the magnitude increases in turn, especially at low frequencies, while the Italian relation attenuates more rapidly than the European one at long distances. Thus, looking at Fig. 6 one can expect that

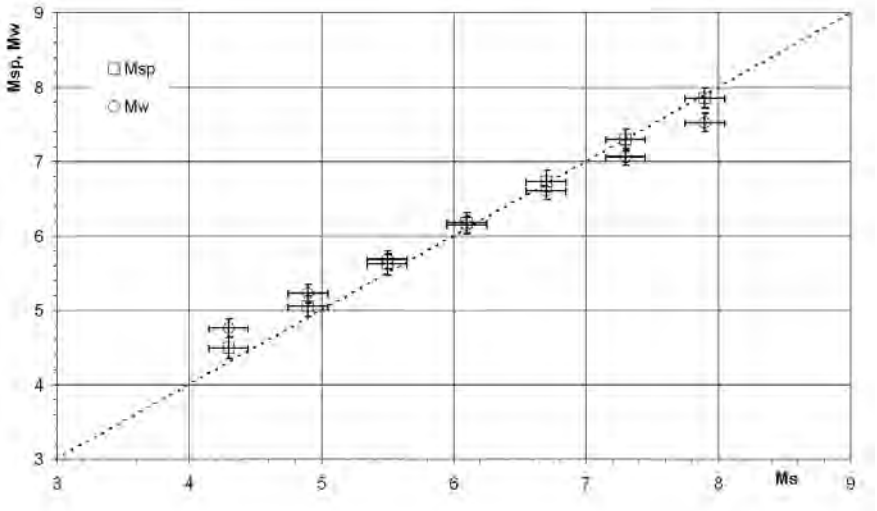

Fig. 5 - Surface wave magnitude (M_S, x-axis) vs. moment magnitude (M_W, y-axis) and hybrid magnitude (M_{SP}, y-axis) (source data from MPS04). *Msp* is used in the Italian attenuation relationships with the meaning of local magnitude below *M*5.5 and surface wave magnitude above it. Error bounds clearly show that no conversion is needed to transform *Msp* into *Ms*, while a conversion relation is needed to transform *Mw* into *Ms*. This is why we used only attenuation relationships based on surface waves magnitude, in order to avoid further uncertainties due to magnitude conversions to be properly accounted for.

the Italian relation does provide more conservative hazard values than the European one for long return periods and short source-to-site distances, i.e., for the spatially-concentrated seismic source model.

6. Logic-tree structure and constrains

At this point, the state of the nature that is consistent with the Reference Seismicity may be organised in a logic-tree structure that is shown in Fig. 7.

This structure implies 12 independent branches, each one repeated for three return periods and three spectral periods, for a total of 108 hazard estimates and maps. The return periods investigated are 100, 500 and 1000 years: they provide the seismic actions for, respectively, Occasional, Rare and Very Rare earthquakes to be used in the Performance-Based Earthquake Engineering (PBEE) design (Porter, 2003) for, respectively, Operational, Life Safe and Near Collapse performance objectives and related to the damage and ultimate limit states design for ordinary and critical structures. Furthermore, the three return periods are the only ones that can be reliably predicted. In fact, they correspond, respectively, to the shortest completeness interval, to the longest one and to the time-span covered by the whole earthquake catalogue. Any hazard estimate exceeding the millennium represents an extrapolation that usually leads to uncontrolled and perhaps unrealistic, very strong values of ground motion (Brune, 1996).

The three spectral periods investigated are peak ground acceleration (PGA) and spectral accelerations (SA) at 5 Hz (SA5) and 1 Hz (SA1) for a 5% of the critical damping. 5 and 1 Hz represent the average frequencies where the maximum response in, respectively, acceleration and

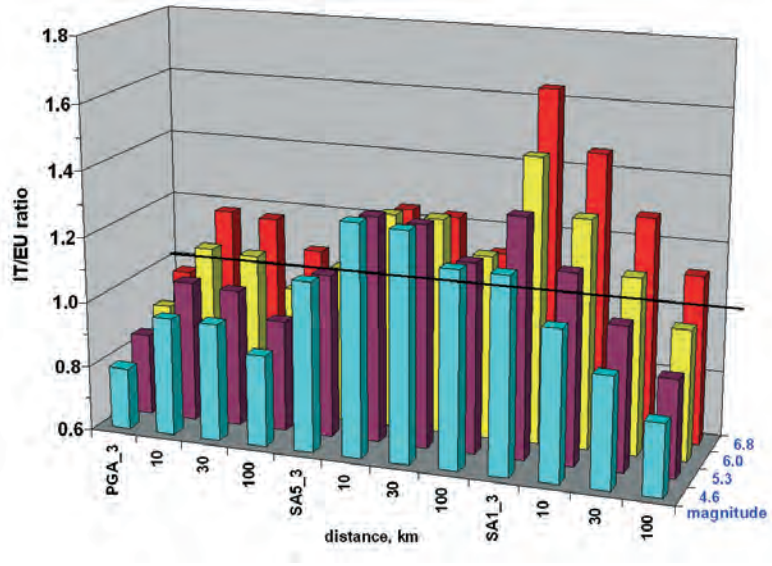

Fig. 6 - Ratio of the strong motion values predicted by the Italian versus European attenuation relationships, as a function of magnitude and distance. On the distance axis the three ground motion parameters investigated in this study are reported: horizontal PGA; horizontal SA5 and SA1.

velocity can be observed on stiff reference soil conditions (Prestininzi *et al*., 2005). Thus, three spectral parameters alone (i.e., PGA, SA5, SA1), completely describe a code-like spectrum up to the beginning of the branch of constant displacement (Newmark and Hall, 1982; Prestininzi *et al*., 2005).

In order to assign a degree of belief for each branch, a holistic process of elicitation of a pool of experts has been achieved (Roberds, 1990). About one-fourth of the solicited experts (14 out of 52) answered a questionnaire where a judgement about the reliability of each choice was asked. The results are shown in Fig. 8.

The most voted path was "Seismic-zones → GR law → Italian attenuation", with a relative

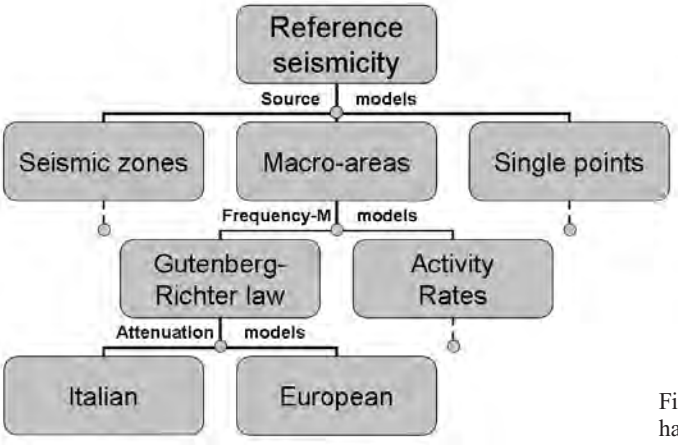

Fig. 7 - Logic-tree structure used in the seismic hazard analysis.

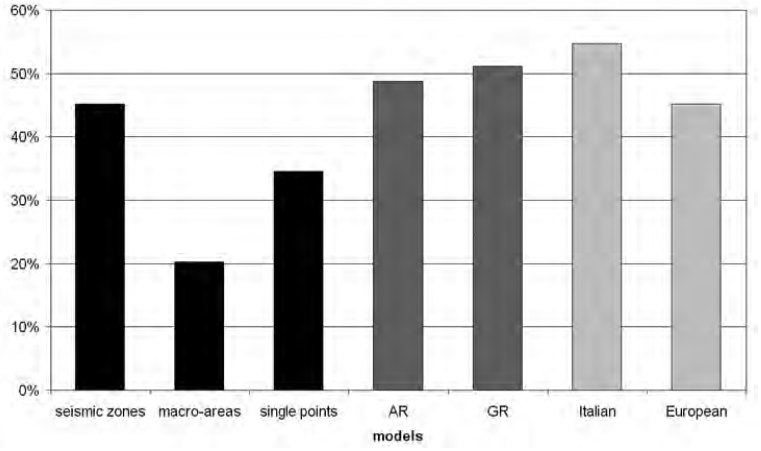

Fig. 8 - Degree of belief expressed by a panel of seismic hazard experts for each model implemented in this study (see the logic-tree structure shown in Fig. 7).

possibility of 13%, and the less voted was "Macro-areas → AR → European attenuation", with a relative possibility of 4%.

7. Hazard maps and sensitivity analyses

Fig. 9 gives an example of the different seismic hazard maps obtained using alternative seismicity models as those shown in the logic-tree structure adopted in this study (Fig. 7). It is worth observing that GR rates estimate lower hazard values than AR rates; this evidence was already pointed out by Romeo and Pugliese (2000) and is related to the lower *b*-values that are computed in the smallest zones of southern Italy. Thus, while AR rates follow the observed distribution of the seismicity in each zone, GR rates smooth them with a *b*-value fixed to 1. In the same way Fig. 10 shows, for one single model combination, what can be observed by changing the period of observation (i.e., the return period) or the frequency bandwidth (i.e., the ground motion spectral parameter). Of course, figures are far from exhaustive with respect to the influence exerted by the alternative models implemented in this study; for instance, the hazard map produced by the macro-area seismic source model is not shown, since ground motion values are clearly spread over large areas with relatively small differences and therefore few are visually representative. Thus, in order to effectively compare the influence exerted by each model on the hazard results, it is surely better to perform a parametric sensitivity analysis. To this aim, we first derived a reference motion given by the average of the twelve spectral accelerations at 5 Hz and return period of 500 years computed through the twelve alternative models. Then, having fixed one model for source, rate or attenuation, we computed the mean value of SA5 for a 500-year return period from all the branches of the other nodes of the logic-tree structure (Fig. 7). Thus, for each source model, we computed the mean of four SA values, derived from 2x2 rates and attenuation models; for each rate model (GR and AR), we computed the mean of six SA values, derived from 3x2 source and attenuation models; and finally, for each attenuation model, we computed, six SA values again, derived from 3x2 source and rates models.

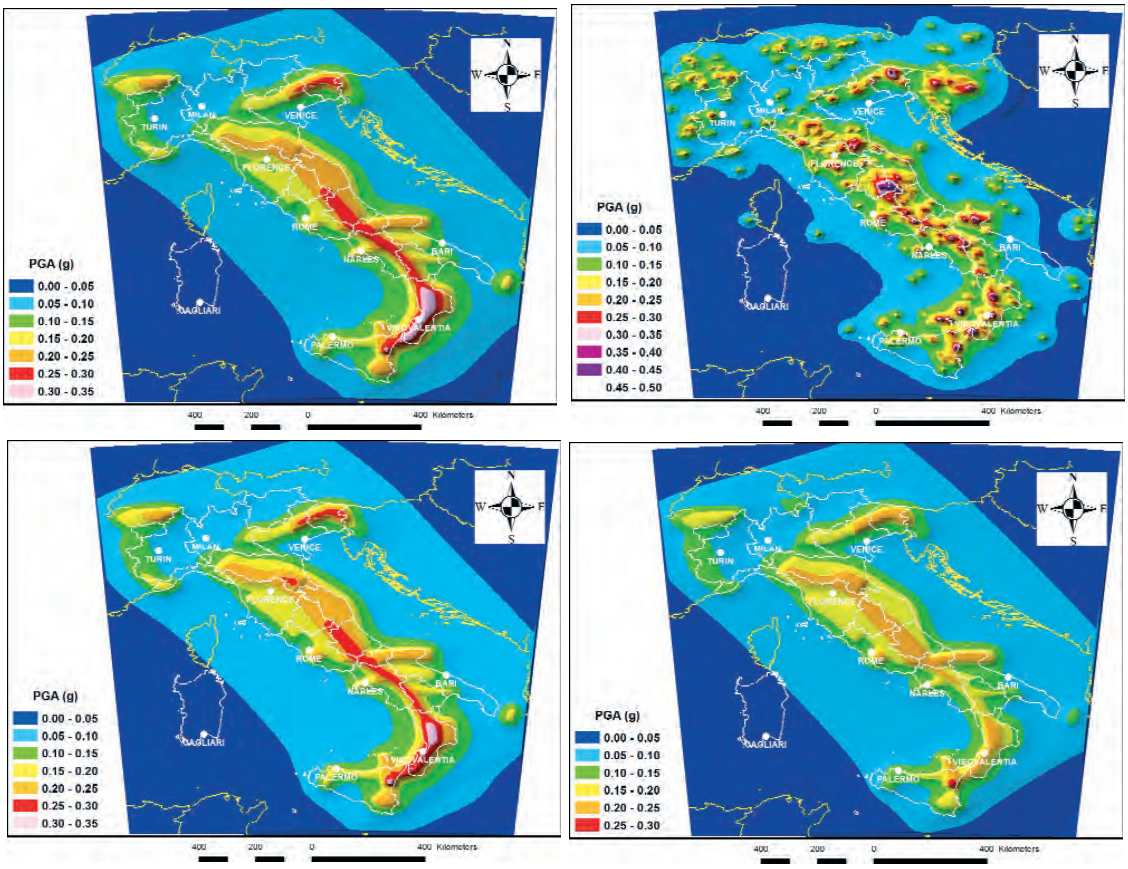

Fig. 9 - Seismic hazard maps in PGA-values expected with a return period of 500 years for some alternative models implemented in the logic-tree structure (Fig. 7). Upper-left: Seismic zones + AR + Italian attenuation. Upper-right: Single points + AR + Italian attenuation. Bottom-left: Seismic zones + AR + European attenuation. Bottom-right: Seismic zones + GR + Italian attenuation. Maps on the top compare two out of three source models. Maps on the left compare the two attenuation models. On the diagonal (from top-left to bottom-right) are compared the two seismicity rate models.

For the comparison, we chose the SA values at 5 Hz because they determine the constant acceleration branch of the code-like response spectrum, which is of primary importance for the engineering design of structures. Fig. 11 shows the results of the parametric sensitivity analyses.

Regarding the attenuation models, it can be seen that the influence is within a ±10% difference, with the Italian attenuation relationship predicting ground motion values that are more conservative than the European ones. A slight increase of the divergence between the two models can be observed as the hazard increases (i.e. as the reference ground motion values increase).

Regarding the seismicity rate models the influence is less pronounced than in the previous case, ranging within ±5%. Anyway, the AR model predicts ground motion values slightly greater than the GR model as the site hazard increases.

As expected, the strongest influence on the hazard results is exerted by the source models. The macro-areas and single-point models, with an opposite trend, determine the extreme hazard values: the macro-area model overestimates the ground motion values for low hazard sites and

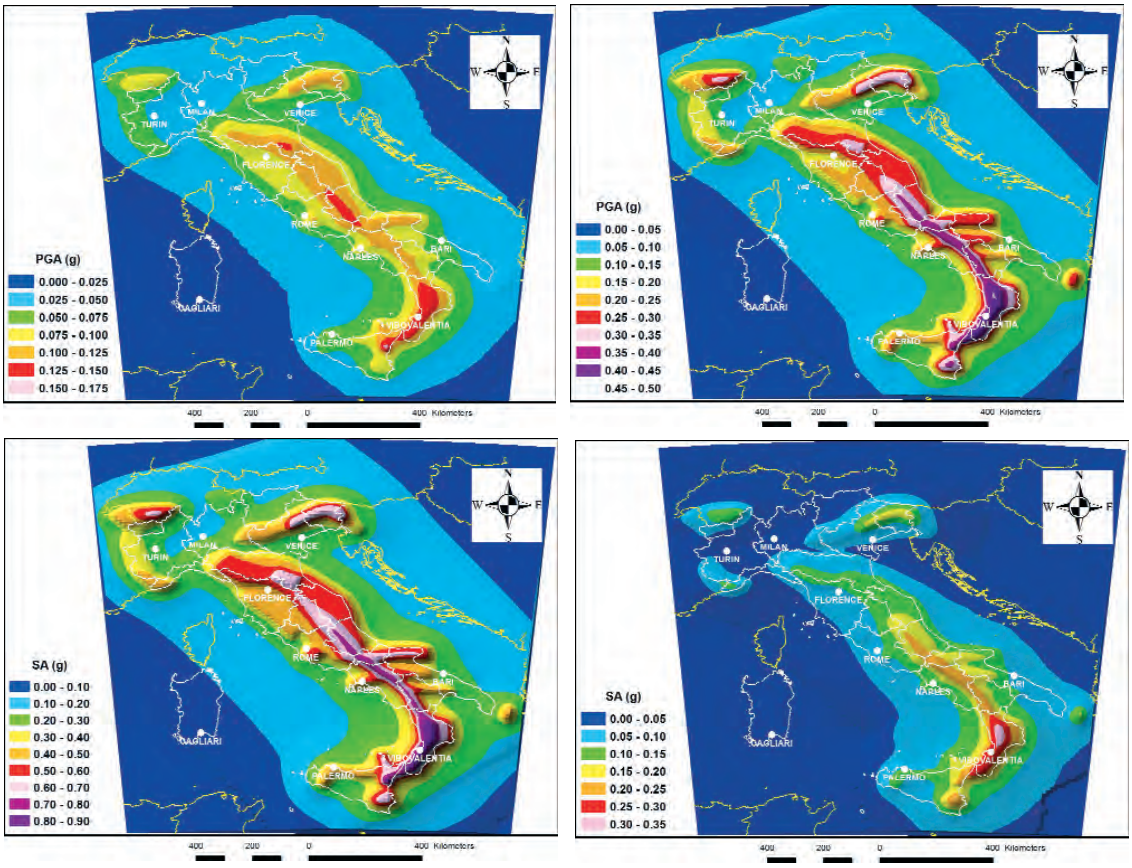

Fig. 10 - In the first row, seismic hazard maps for PGA-values expected with a return period of 100 years (top-left) and 1,000 years (top-right). In the second row, spectral acceleration values at 5 Hz (bottom-left) and 1 Hz (bottom-right) expected with a return period of 500 years. All the maps refer to the following model combinations: Seismic zones + AR + Italian attenuation. Maps of SA5 and PGA with a 100-years return period have scales that are, respectively, twice and one-half that of the other maps.

underestimates them for high hazard sites; the reverse is true for the single-point model. The reason is that the macro-area model distributes earthquakes in wide areas, thus increasing the hazard even where the historical catalogue reports no earthquake. On the contrary, the single-point model concentrates earthquakes just where the earthquake catalogue locates them. Ultimately, the macro-area model increases the hazard of low seismic regions and depresses that of high seismic regions; the single-point model exalts the hazard of high seismic regions and reduces that of low seismic regions; the seismic-zones model operates a smoothing of the overall hazard and it just represents a compromise between the previous models.

8. Validation tests

Each one of the twelve hazard outcomes (the twelve end-branches of the logic-tree structure) is a possible hazard scenario or realization of a state of nature; one is no more likely to occur than

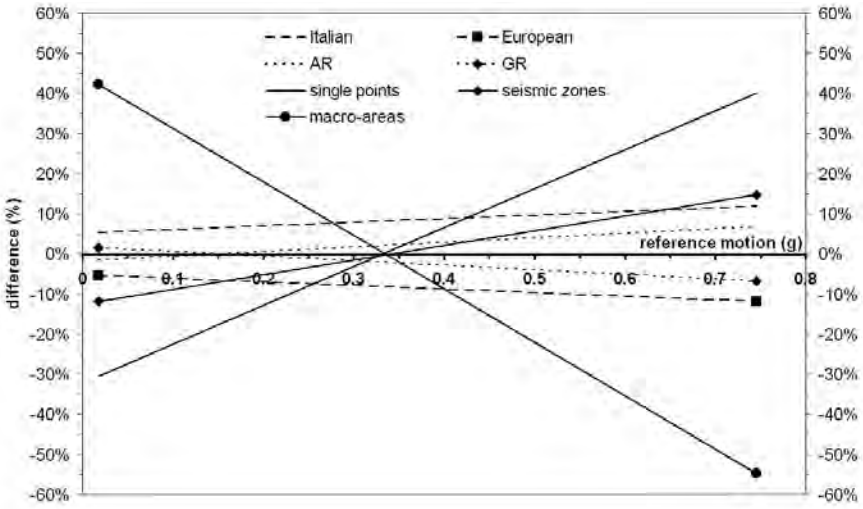

Fig. 11 - Influence exerted on the hazard analyses by each model displayed as differential trends with respect to a reference motion. The reference motion is given by the average of the spectral accelerations (at 5 Hz) of all the alternative models. Then for each model, the average of the spectral accelerations coming from all the branches departing from the other nodes of the logic-tree is computed and plotted as linear trend of the algebraic difference with the reference motion. A positive difference means that the model is contributing more than the alternative one(s); the reverse is true for negative differences.

another one. But, may we determine if one of them is more reliable than another one? If we skip the subjective judgements of a holistic process (previously shown), the only way is to compare them with an independent hazard estimate that we assume to be true or, at least, the most reliable. Since the hazard estimates we have shown are assessed by an indirect approach (from source to site), we need to assume, as reference hazard, an estimate based on a direct approach, that means, a site hazard approach. As known, there are not enough strong-motion records to compute a site hazard covering the entire country and spanning a long time-window; nevertheless a long record of felt intensities for a large number of sites is available. To this aim, we used a study of Albarello and D'Amico (2001) who computed the yearly occurrence of site intensities for the Italian municipalities based on over 36,000 historically documented felt intensities. For 2579 out of 8100 Italian municipalities, we were able to compute the expected site intensity with a return period of 500 years from the original data of Albarello and D'Amico (2001). The expected site intensities range between VI and X-XI degrees of the MCS scale. Now, the key question is: how may we compare hazard estimates in site intensities with hazard estimates in ground motion values? To do this we would need a correlation equation between intensity and a ground motion parameter such as PGA, PGV or something else. In literature, there are many equations (Chiaruttini and Siro, 1981; Margottini *et al*., 1992; Faccioli and Cauzzi, 2006), but all of them are affected by considerable uncertainties. To bypass this problem, we ranked the hazard estimates for those municipalities having both a site intensity and a ground motion hazard. Now, we had an unbiased set of data to compare objectively the two hazard estimates without applying any unreliable conversion equation. Fig. 12 shows the site intensity hazard estimates ranked in a normalized scale between 0 (the lowest hazard value) and 1(the highest hazard value).

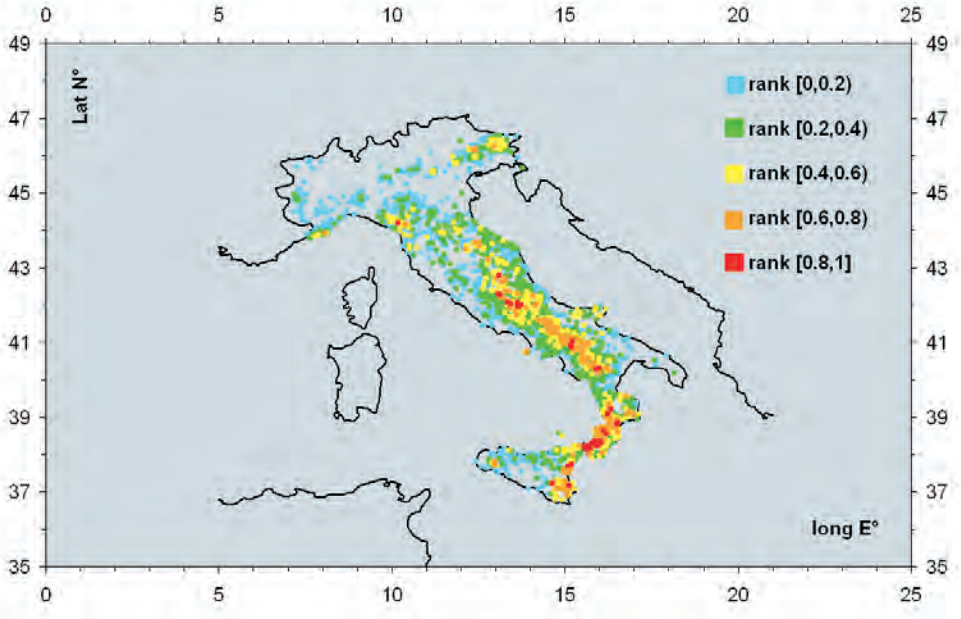

Fig. 12 - Site intensities computed from the work of Albarello and D'Amico (2001) with a 500-year return period. The values refer to 2579 municipalities and they have been ranked from 0 to 1 for the purpose of comparison with the ground motion estimates of the hazard analyses. Square bracket shows that class limit is included; round bracket indicates that class limit is not included.

We observe, that despite the fact that the number of sites is less than one third of the Italian municipalities, they cover anyway most of the country and they are located in the most active regions (see for comparison Fig. 2) where the hazard has to be more reliably estimated. Two ranking tests were performed, the first based on a classical variance analysis:

$$VAR = \frac{\sum_{i=1}^{n}\left[R'(X_i) - R'(Y_i)\right]^2}{(n-1)}, \tag{2}$$

and the second one based on a rank correlation coefficient (Spearman's coefficient):

$$\rho' = 1 - \frac{6\sum_{i=1}^{n}\left[R(X_i) - R(Y_i)\right]^2}{n\left(n^2-1\right)}. \tag{3}$$

The former is a measure of the absolute difference among ranks, where R' means that ranks have been normalized from 0 to 1. The latter expresses the similarity between the two sets of rankings and, analogously to the ordinary correlation coefficient ρ', it varies from 0 (no correlation) to 1 (perfect correlation): a ρ' lower than 0.5 indicates a weak correlation between the two data sets, whereas a ρ' greater than 0.5 suggests a meaningful correlation. We compared

the ranks of site intensity with those of the spectral acceleration at 1 Hz; the choice of SA1 is dictated by its better correlation with damage than PGA or SA5 (see Table 2 for the results of the validation tests).

From the table, sorted by decreasing values of Spearman's coefficient, one can infer that the seismic source models play the most important role. The single point model achieves the best correlation and agreement with the observed hazard independently from the seismicity rate model or the attenuation relationship; on the contrary, the seismic zone model becomes more meaningful if the AR seismicity rate model is implemented, independently from the adopted attenuation model. The AR seismicity model ranks a little bit higher than the GR model, such as the Italian attenuation model is slightly more consistent with the observed hazard than the European one especially in the case of concentrated seismicity, as already pointed out in the attenuation section of this paper. The last column shows the results of the questionnaire sent to the Italian seismic hazard experts; though they show a general, good agreement with the results of the statistical tests, it is nevertheless worth noting that the highest degree of belief is placed in a models' combination that occupies the lower half of the rank in both the statistical tests.

9. Final remarks

The results achieved in this study have more than one implication as regards the approach to the seismic hazard. First of all, any seismic hazard study must start fixing the reference seismicity, i.e., the reference, yearly number of earthquakes above the magnitude of engineering interest. After that, a set of alternative models can be consistently formulated and their influence on the hazard results explored. Any model is a possible hazard scenario, whose reliability should

Table 2 - Results of the statistical tests carried out for the twelve models of seismic hazard. The comparison has been made with the ranked values of site intensity hazard shown in Fig. 11. The last column reports the degrees of belief expressed by the seismic hazard experts interviewed in this work.

Model	Spearman's coefficient	Variance	Degree of belief
Seismic zones + AR + Italian attenuation	0.605	0.0627 (5°)	12%
Seismic zones + AR + European attenuation	0.601	0.0665 (6°)	10%
Single points + AR + Italian attenuation	0.522	0.0422 (3°)	9%
Single points + GR + Italian attenuation	0.519	0.0481 (4°)	10%
Single points + AR + European attenuation	0.518	0.0394 (1°)	8%
Single points + GR + European attenuation	0.515	0.0419 (2°)	8%
Seismic zones + GR + Italian attenuation	0.468	0.1452 (9°)	13%
Seismic zones + GR + European attenuation	0.456	0.1529 (10°)	10%
Macro-areas + AR + Italian attenuation	0.405	0.1258 (8°)	5%
Macro-areas + AR + European attenuation	0.401	0.1250 (7°)	4%
Macro-areas + GR + European attenuation	0.152	0.2620 (11°)	5%
Macro-areas + GR + Italian attenuation	0.148	0.2673 (12°)	6%

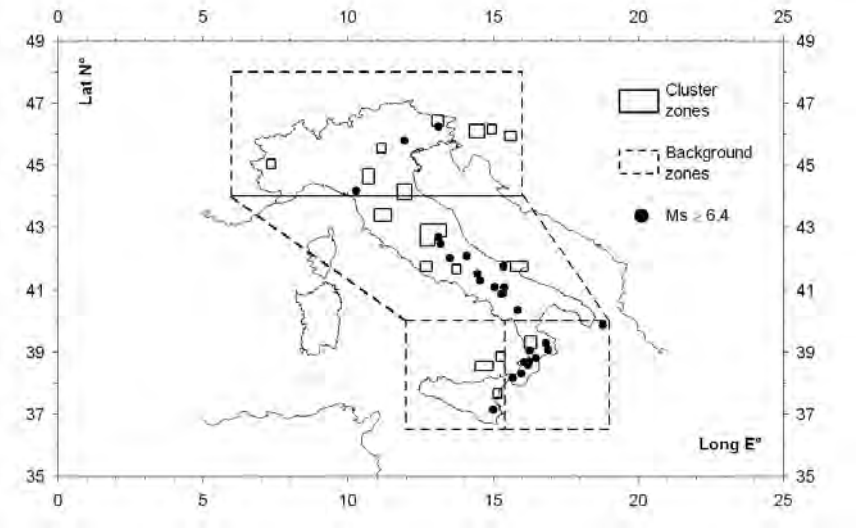

Fig. 13 - Seismic source models implemented for the computation of the best hazard.

be always proved and whose choice depends on the desired effect or on the use that must be made of it. For instance:

1) The seismic zoning of the country depends strictly on the source model adopted for the hazard study. Thus, if one wants to privilege a widespread seismic classification of the country, one should adopt the macro-areas model. The source models by zones and single points emphasize the relevance of the highest seismic zones.

2) The frequency content of the hazard spectra are controlled instead by seismicity rates and attenuation models. The European attenuation equation provides the highest PGA values while the highest spectral accelerations at 1 and 5 Hz are given by the Italian attenuation relationships; the AR model usually predicts higher spectral values than the GR model, especially when associated to concentrated source models, and vice versa.

Thus, depending on the final use of the hazard analyses (e.g., risk analyses, seismic zoning of the country, earthquake engineering design purposes), one branch of the logic-tree structure may be more suitable than another one.

Moreover, the sensitivity analyses and validation tests suggest that there could be some preferred combinations among the models, for example, the more concentrated the source, the more appropriate an activity rate (AR) model rather than the GR one. Thus a reference hazard, as a summary and consistent with these and further evidence, has been achieved based on:

1. single points for earthquake magnitude equal to or greater than 6.4, accounting for a characteristic earthquake occurrence model (Wesnousky, 1994);
2. small zones of concentrated seismicity based on a spatial clustering of earthquakes below M=6.4, whose seismicity rates are described by an AR model (observed rates);
3. background areas of diffuse seismicity set to face any non-stationarity in the spatial distribution of earthquakes, following a GR seismicity rate model.

The clustering process adopted in this study consists of mobile spatial windows with a cell spacing of 0.2° degrees in latitude and longitude and stepping 0.1° in both directions. The clusters

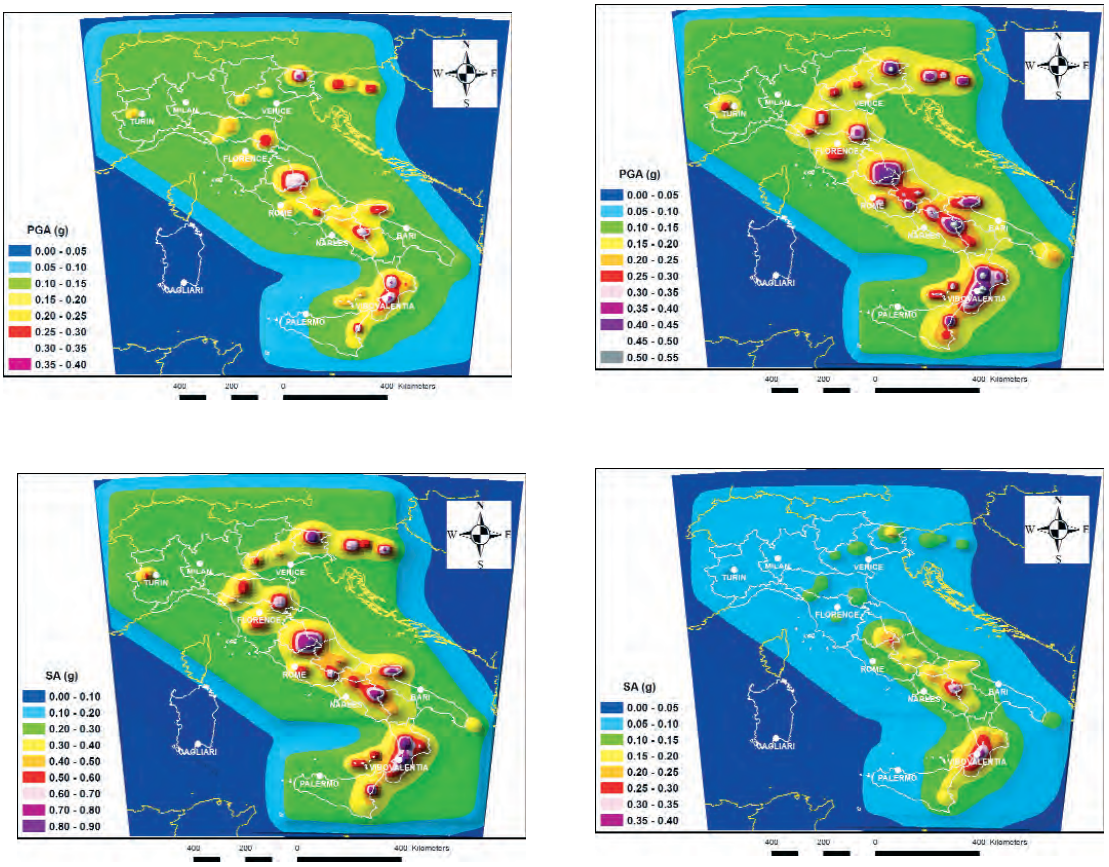

Fig. 14 - Hazard of best-estimate. Maps displayed are: on the top, PGA with 500-(left) and 1,000-(right) year return periods; on the bottom, SA5 (left) and SA1 (right) with a return period of 500 years.

are selected grouping together those nearby cells containing three or more earthquakes (corresponding to the average + one standard deviation number of earthquakes per cell). The source model adopted is shown in Fig. 13.

Then, we averaged the ground motion predictions of both Italian and European attenuation relationships with a random uncertainty (in log-units) of 0.3 and we incorporated also the intrinsic uncertainty of the magnitude-frequency distributions and that on the seismic sources' boundaries, in order to take the aleatory nature of the seismic hazard uncertainty completely into account.

For the sake of homogeneity, Fig. 14 shows our best-estimate PGA and SA hazard maps for different return periods, whereas Fig. 15 shows the trends of the short-period spectral amplification and of the period at which the constant velocity branch of the spectrum begins. The statistical tests carried out for the best estimate according to the procedure described in the previous section of this paper, gave a variance of 0.034 and a Spearman's coefficient of 0.6. This turns out a little-bit better than the best model shown in Table 2, thus justifying it as best-estimate, but still not sufficiently satisfactory as expected and this is the reason why a further study, just in progress, is envisaged with the aim of improving the correlation with the observed spatial and

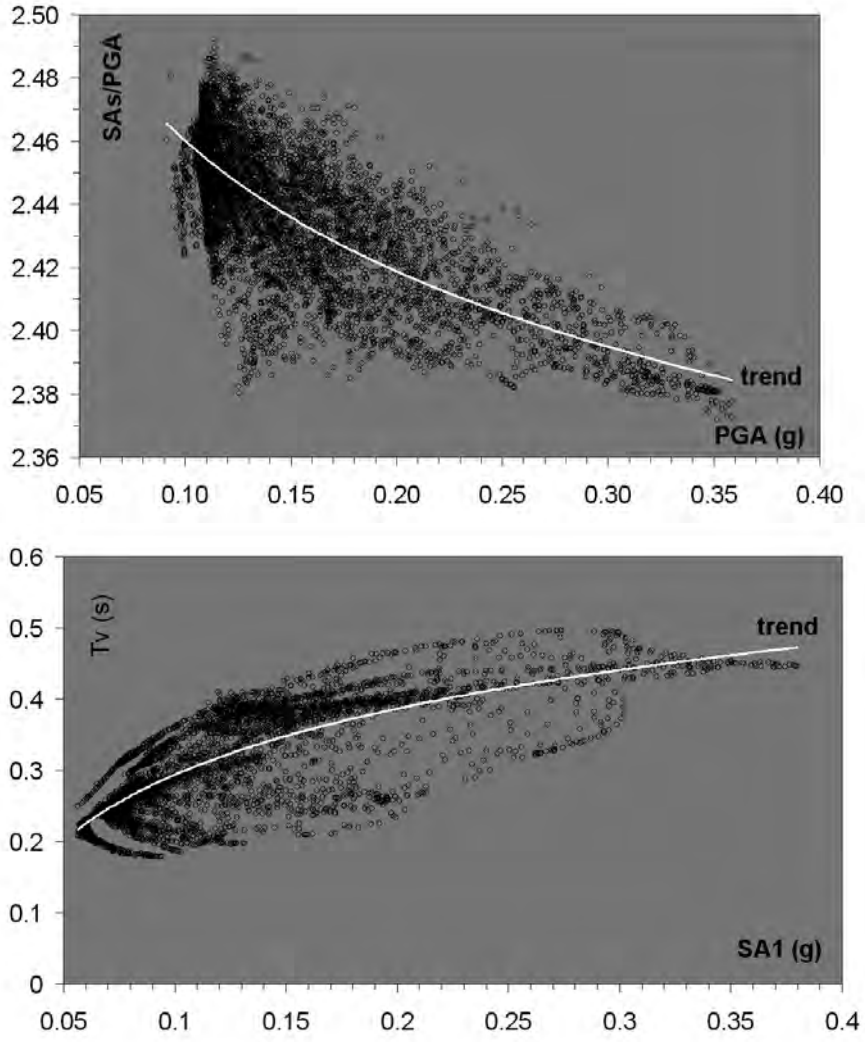

Fig. 15 - Upper panel: trend of the spectral acceleration amplification coming from the best-estimate hazard. Lower panel: the same as before but for the spectral period marking the beginning of the constant velocity branch of the design spectrum.

temporal occurrence of the seismicity.

From the figures above, we can make some concluding remarks concerning the effects of such a hazard on the seismic classification of the country, as well as on the seismic rules for the engineering design of structures.

First, looking at the hazard map one can infer that the whole country of Italy – except for the island of Sardinia – should be classified at least in the third seismic zone (low seismicity, PGA-values between 0.05 g and 0.15 g). The effect of spreading ground motion values over large regions is the result of adopting background areas, which account for any kinds of non-stationarity in the spatial distribution of earthquakes and which often represents the largest source of uncertainty in every seismic hazard model. This creates wide regions of constant acceleration

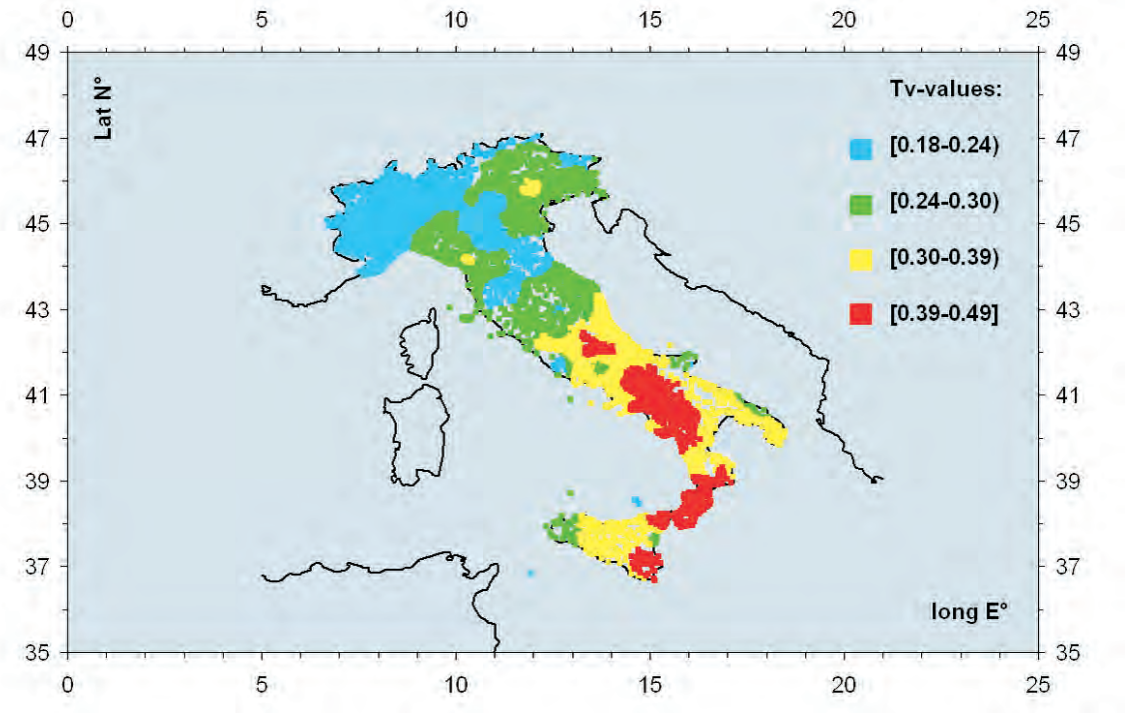

Fig. 16 - Distribution of *Tv*-values, i.e., the spectral period (in seconds) when the constant velocity branch of the spectrum starts.

and 'hot-spots' of concentrated seismicity (cluster-zones and single-points with $M \geq 6.4$) where hazard concentrates, each type accounting for a spatial uncertainty in its location.

Secondly, the code-like spectrum has a shape, depending on the seismicity level of the site, as pointed out by Prestininzi *et al*. (2005). In particular, the greater the hazard the lower the maximum amplification in the constant acceleration branch of the spectrum; conversely, the lower the hazard the narrower the constant acceleration branch. Moreover, the period (*Tv*) when the constant velocity branch of the spectrum starts, is controlled by the low-frequency values (SA1) and, ultimately, by the maximum expected magnitudes. In fact, the magnitude coefficients of both the attenuation relationships used in this study increase as the spectral period increases itself. Thus, we observe the maximum *Tv*-values in the most hazardous areas (see Fig. 16 to be compared, for reference, with the SA1 hazard map displayed in Fig. 14). Actually, low seismic hazard sites are characterized by narrower but higher amplified spectra than those pertinent to high seismic hazard sites. As an example, Fig. 17 displays the design spectra for two sites located in high seismic areas (Vibo Valentia) and in low seismic areas (Venice).

According to Prestininzi *et al*. (2005), the spectral period when the constant acceleration branch of the spectrum starts is worth:

$$Tv = SA_{1\text{Hz}}/SA_{5\text{Hz}}, \tag{4}$$

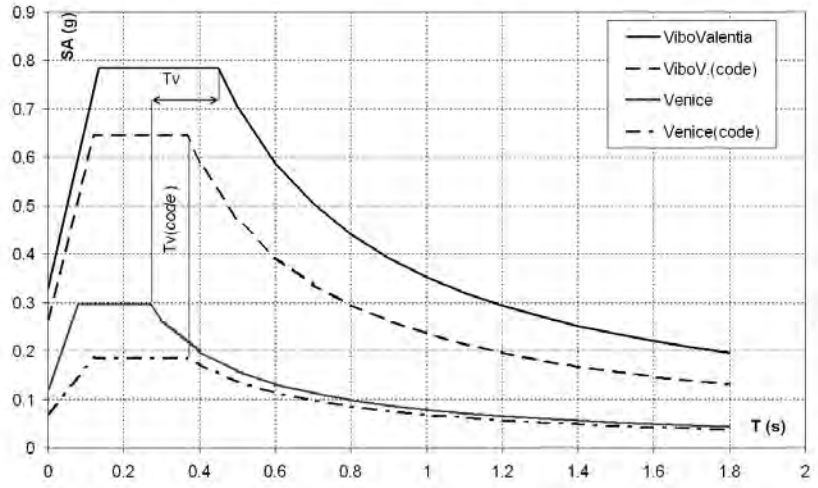

Fig. 17 - Code-like spectra for two sites, one located in a high seismic area (Vibo Valentia) and the other one located in a low seismic area (Venice). For comparison the same spectra provided by the current Italian seismic code (Ministry of Infrastructures, 2008) are also plotted (labelled as code). *Tv* is the spectral period when the constant velocity branch of the response spectra begins.

(provided that SA1 is the maximum spectral velocity), whereas the minimum spectral period corresponding to the beginning of the constant acceleration branch is worth:

$$0.06 \text{ s} \leq Ta \approx Tv * 0.3 \leq 0.2 \text{ s}. \quad (5)$$

The figure also displays the spectra for the same sites provided by the current seismic code (Ministry of Infrastructures, 2008), that derived the seismic actions from the MPS04 (2004) seismic hazard analysis. It is worth mentioning that the sites are equally ranked in this study as well as to the MPS04 (2004) study as belonging to, respectively, high and low seismic zones. Apart from the different spectral acceleration values, which depend on the reference seismic hazard used, what is surprising is that for the seismic code two sites with a very different hazard level have the same width of the constant acceleration branch and in the same frequency interval.

On the contrary, our approach respects the condition that the higher the hazard the greater the spectral period when the constant velocity branch begins, according to the fundamental Newmark-Hall's (1982) study.

The concluding remark of this work is that any hazard assessment cannot avoid exploring the nature and effects of the multiple sources of uncertainty prior to reaching a result consistent with all the available observations, and in this sense we leave the last word to Susan Hough who, in her appreciable book "Earthshaking Science" edited by the Princeton University Press (NJ), states that

Like any system science, hazard mapping isn't simply a puzzle to be solved but a mélange of multiple puzzles, each to be solved in its own right and then finally fit together.
(Susan Elizabeth Hough, 2002)

Acknowledgments. This paper reflects the contents of an invited talk held in November 2007 at the 26th Annual Congress in Geophysics of the Solid Earth, session "2.2 Seismic Characterization of the Territory". The authors wish to thank the session's chairpersons D. Albarello and G. Naso for their helpful comments and suggestions. GISLab (www.uniurb.it/gislab/) provided tools and know-how in achieving the seismic hazard maps. The authors acknowledge the following experts in seismic hazard who contributed to the compilation of the questionnaire: D. Albarello, S. Barba, M.S. Barbano, A. De Sortis, A. Goretti, M. Mucciarelli, G. Naso, A. Paciello, L. Peruzza, A. Prestininzi, F. Sabetta and three experts who asked to remain anonymous. Their contribution as well as that of any other person who either directly or indirectly contributed to the present work is particularly appreciated. D. Albarello and F. Sabetta reviewed the manuscript and their helpful comments improved the paper very much.

REFERENCES

Abrahamson N.A. and Bommer J.J.; 2005: *Probability and uncertainty in seismic hazard analysis.* Earthq. Spectra, **21**, 603-607.

Akinci A.; 2004: *Applicazione del metodo a sismicità diffusa.* In: MPS04, appendix 4. http://zonesismiche.mi.ingv.it/.

Albarello D.; 2006: *Alberi logici e non: la propagazione delle incertezze nella stima della pericolosità sismica con metodi probabilistici.* In: Slejko D. and Rebez A., (eds), Gruppo Nazionale di Geofisica della Terra Solida, 25° Convegno Nazionale, Riassunti estesi delle comunicazioni, Stella Arti Grafiche, Trieste, pp. 205-208.

Albarello D. and D'Amico V.; 2001: *Sviluppo di metodologie innovative per il calcolo della pericolosità sismica del territorio nazionale.* SSN Report, Rome.

Albarello D., Bosi V., Bramerini F., Lucantoni A., Naso G., Peruzza L., Rebez A., Sabetta F. and Slejko D.; 2000: *Carte di Pericolosità sismica del territorio nazionale.* Quad. Geof., **12**, 1-8.

Albarello D., Bramerini F., D'Amico V., Lucantoni A. and Naso G.; 2002: *Italian intensity hazard maps: a comparison of results from different methodologies.* Boll. Geof. Teor. Appl., **43**, 249-262.

Ambraseys N.N., Simpson K.A. and Bommer J.J.; 1996: *Prediction of horizontal response spectra in Europe.* Earthq. Eng. Str. Dyn., **25**, 371-400.

Ambraseys N.N., Douglas J., Sarma S.K. and Smit P.M.; 2005: *Equations for the estimation of strong ground motions from shallow crustal earthquakes using data from Europe and the Middle East: horizontal Peak Ground Acceleration and Spectral Acceleration.* Bull. of Earthq. Eng., **3**, 1-53.

Brune J.N.; 1996: *Precariously balanced rocks and ground-motion maps for Southern California.* Bull. Seism. Soc. Am., **86**, 43-54.

Caputo M.; 2000: *Comparison of five independent catalogues of earthquakes of a seismic region.* Geoph. J. Int., **143**, 417-426.

Chiaruttini C. and Siro L.; 1981: *The correlation of peak ground horizontal acceleration with magnitude, distance, and seismic intensity for Friuli and Ancona, Italy, and the Alpide Belt.* Bull. Seism. Soc. Am., **71**, 1993-2009.

Cornell C.A.; 1968: *Engineering seismic risk analysis.* Bull. Seism. Soc. Am., **58**, 1583-1606.

Faccioli E. and Cauzzi C.; 2006: *Macroseismic intensities for seismic scenarios estimated from instrumentally based correlations.* In: Proc. 1st Eu. Conf. on Earthq. Eng. and Seismol., paper number 569.

Gutenberg B. and Richter C.F.; 1944: *Frequency of earthquakes in California.* Bull. Seism. Soc. Am., **34**, 1985-1988.

CPTI 04; 2004: *Catalogo Parametrico dei Terremoti Italiani.* http://emidius.mi.ingv.it/CPTI04/.

CSI 1.1; 2006: *Catalogo della Sismicità Italiana (1981-2002).* http://legacy.ingv.it/CSI/.

Krinitzsky E.L.; 1995: *Problems with logic trees in earthquake hazard evaluation.* Eng. Geol., **39,** 1-3.

Margottini C., Molin D. and Serva L.; 1992: *Intensity versus ground motion: a new approach using Italian data.* Eng. Geol., **33**, 45-58.

McGuire R.K.; 2004: *Seismic hazard and risk analysis.* EERI Monograph, **10**, Berkeley, CA.

Meletti C., Patacca E. and Scandone P.; 2000: *Construction of a seismotectonic model: the case of Italy.* Pure and Appl. Geophy., **157**, 11-35.

Ministry of Infrastructures; 2008*: Norme Tecniche per le Costruzioni.* G.U., **29**, February 4, 2008.

Montone P., Pondrelli S., Amato A., Mariucci M.T. and Pierdominici S.; 2003: *An improved stress map of Italy and Central Mediterranean.* In: EGS-AGU-EUG Joint Assembly 2003, Geophy. Res. Abs., 5, 10362.

MPS04; 2004: *Redazione della mappa di pericolosità sismica prevista dall'OPCM 3274.* INGV Report, 65 pp., 5 appendices. http://zonesismiche.mi.ingv.it/

Newmark N.M. and Hall W.J.; 1982: *Earthquake spectra and design.* EERI Monograph, **3**, Berkeley, CA.

NTC 2005: *Norme Tecniche per le Costruzioni.* G.U., **222**, September 23, 2005.

OPCM 2788; 1998: *Individuazione delle zone ad elevato rischio sismico del territorio nazionale.* G.U., **146**, June 25, 1998.

OPCM 3274; 2003: *Primi elementi in materia di criteri generali per la classificazione del territorio nazionale e di normative tecniche.* G.U., **105**, May 8, 2003.

Orsini G.; 1999: *A model for buildings' vulnerability assessment using the Parameterless Scale of Seismic Intensity (PSI).* Earthq. Spectra, **15**, 463–483.

Porter K.A.; 2003: *An overview of PEER's performance-based earthquake engineering methodology.* In: Proc. 9° ICASP in Civ. Eng., **2**, 973-980.

Prestininzi A., Pugliese A. and Romeo R.W.; 2005: *Proposed seismic classification of Italy and related seismic actions*. It. J. Eng. Geol. Env., **1**, 57-70.

Reiter L.; 1990: *Earthquake hazard analysis.* Columbia University Press, New York, NY.

Roberds W.J.; 1990: *Methods for developing defensible subjective probability assessments.* Transp. Res. Rec., **1288**, 183-190.

Romeo R.W. and Pugliese A.; 2000: *Seismicity, seismotectonics and seismic hazard of Italy.* Eng. Geol., **55**, 241-258.

Romeo R.W., Paciello A. and Rinaldis D.; 2000: *Seismic hazard maps of Italy including site effects.* Soil Dyn. and Earthq. Eng., **20**, 85-92.

Sabetta F. and Pugliese A.; 1996: *Estimation of response spectra and simulation of nonstationary earthquake ground motions.* Bull. Seism. Soc. Am., **86**, 337-352.

Scandone P. and Stucchi M.; 2000: *La zonazione sismogenetica come strumento per la valutazione della pericolosità sismica*. In: Galadini F., Meletti C. and Rebez A. (eds), Le ricerche del GNDT nel campo della pericolosità sismica (1996-1999), CNR/GNDT Monograph, Rome, pp. 3-14.

Slejko D., Peruzza L. and Rebez A.; 1998: *Seismic hazard maps of Italy.* Ann. Geof., **41**, 183-214.

Vai G.B.; 2001: *Structure and stratigraphy: an overview.* In: Vai G.B. and Martini I.P. (eds), Anatomy of an orogen. The Apennines and adjacent Mediterranean basins. Springer, pp. 15-32.

Valensise G. and Pantosti D.; 2001: *Database of potential sources for earthquakes larger than M 5.5 in Italy.* Ann. Geof., **44**, 180 pp., with CD-ROM.

Wesnousky S.G.; 1994: *The Gutenberg-Richter or characteristic earthquake distribution, which is it?* Bull. Seism. Soc. Am., **84**, 1940-1959.

Corresponding author: Roberto W. Romeo
GISLab, IT Resources for Natural Hazards
University Carlo Bo
Sogesta Scientific Campus, 61029 Urbino (Italy)
phone: +39 0722 304235; fax: +39 0722 304260; e-mail: rwromeo@yahoo.it